Single-mode interband cascade lasers emitting below 2.8 μm

Julian Scheuermann, Robert Weih, Michael von Edlinger, Lars Nähle, Marc Fischer, Johannes Koeth, Martin Kamp, and Sven Höfling

Articles you may be interested in

Single-mode interband cascade lasers emitting below 2.8 μm

Julian Scheuermann,[1] Robert Weih,[2] Michael von Edlinger,[1] Lars Nähle,[1] Marc Fischer,[1] Johannes Koeth,[1] Martin Kamp,[2] and Sven Höfling[2,3]

[1]*nanoplus Nanosystems and Technologies GmbH, Oberer Kirschberg 4, Gerbrunn D-97218, Germany*
[2]*Technische Physik, Physikalisches Institut and Wilhelm Conrad Röntgen-Research Center for Complex Material Systems, Universität Würzburg, Am Hubland, Würzburg D-97074, Germany*
[3]*School of Physics and Astronomy, North Haugh, St. Andrews KY16 9SS, United Kingdom*

In this work, single-mode distributed feedback (DFB) interband cascade laser (ICL) devices with record short wavelength emission below 2.8 μm are presented. Pulsed measurements based on broad area laser devices with a cavity of 2 mm length and 150 μm width showed threshold current densities of 383 A/cm^2 at T $= 20\,^\circ$C and a characteristic temperature T_0 of 67 K. Fabricated DFB devices were operated in continuous wave mode at room temperature, with threshold currents of 57 mA and demonstrated side mode suppression ratios of larger than 25 dB. The devices showed current tuning ranges of 7 nm and total (including drive current and temperature) tuning ranges of 12 nm, with respective tuning rates of 21 nm/W, 0.13 nm/mA and 0.29 nm/K. Using the full spectral gain bandwidth of the underlying ICL material, single-mode DFB emission was observed within a wavelength range of 150 nm utilizing different DFB grating periods. © 2015 AIP Publishing LLC.
[http://dx.doi.org/10.1063/1.4918985]

Distributed feedback (DFB) interband cascade lasers (ICLs) with application grade performance have recently become available in the mid-infrared (MIR) spectral range $\sim$3 μm.[1] This makes DFB ICLs interesting for use in tunable laser absorption spectroscopy (TLAS) or other spectroscopic applications, which has already been proven by various experiments.[2–5] A wide variety of chemical and medical applications based on TLAS benefit from these compact and low power consuming laser sources. The further extension of ICL DFB technology regarding wavelength coverage is therefore of high interest, especially also with respect to the performance figures of competing semiconductor laser approaches. Currently, the spectral range around 3 μm can be accessed with semiconductor lasers by three different approaches with reasonable performance[6]: diode lasers based on GaSb using type-I interband-transitions with emission from around 2 to 3.7 μm,[7–11] quantum cascade lasers (QCLs) using intraband-transitions with emission from far-IR to around 3 μm (Ref. 12) and ICLs.[13] The latter use interband-transitions of type-II quantum wells connected in series, which is a hybrid technology between the diode laser and the QCL. ICLs have proven themselves as reliable laser sources in the mid-IR wavelength region from 3 to 6 μm with a performance sweet-spot around 3.6–3.8 μm.[1] Compared to QCLs, ICLs typically have a lower output power but benefit from low threshold current densities and low power consumption.[1,14–16] Spectrally single-mode emission can be implemented in various ways. Based on ICL-material, several approaches like top grating[17] or side grating structures[18,19] have been realized. An approach based on lateral metal gratings as described in Ref. 20 was used for the devices discussed in this work. Continuous wave (cw) ICL operation at room temperature and emission with a wavelength around 2.8 μm is presented, which is so far the shortest ICL emission wavelength reported for ridge waveguide (RWG) and DFB devices. While previously room temperature ICL emission around 2.8–2.9 μm was

published for broad area devices only in pulsed operation,[21,22] we present cw emission at room temperature.

The 5 stage ICL layer structure was grown by solid-source molecular beam epitaxy on a Te-doped GaSb substrate as described in Ref. 15, with the following modifications to the active quantum wells and the injector regions: The layer structure of the W-type quantum well (W-QW) consisted of 2.5 nm AlSb/1.4 nm InAs/3.0 nm Ga$_{0.65}$In$_{0.35}$Sb/1.1 nm InAs/1.0 nm AlSb. The InAs thicknesses of the layers were adjusted with respect to the targeted emission wavelength of $\sim$2.8 μm. The electron injector region was grown with six InAs/AlSb layers with thicknesses of 4.3 nm/1.2 nm, 3.4 nm/1.2 nm, 2.5 nm/1.2 nm, 1.9 nm/1.2 nm, 1.5 nm/1.2 nm, 1.4 nm/2.5 nm, where the five InAs wells closest to the W-QW were highly Si-doped with 6·10^{18} cm^{-3} for carrier rebalancing.[23] Fig. 1 shows the band structure of the conduction and valence band for one and a half stages, containing two W-QWs and the respective hole and electron injector. Also shown are the absolute moduli square of the most important electron (solid lines) and heavy hole (dashed lines) wave functions.

The waveguide comprised 200 nm wide GaSb separate confinement layers (SCL) on both sides of the active region and was embedded between a 2.5 μm lower and a 1.5 μm upper InAs/AlSb superlattice cladding layer. Before and after the SCLs, transition layers were inserted to smoothen out conduction band discontinuities. The doping concentrations in the cladding layers started at 8·10^{17} cm^{-3} on the outside and were reduced to 2·10^{17} cm^{-3} towards the active region. For basic characterization of the epitaxial material, 150 μm wide broad area lasers with cavity lengths of 2 mm were fabricated using optical lithography and chlorine/argon based reactive ion etching (RIE). The etch depth amounted to around 2.3 μm, which corresponds to the beginning of the lower cladding layer. The devices were characterized in pulsed mode (1 kHz, 250 ns) in the temperature range from 10 $^\circ$C to 80 $^\circ$C to extract basic performance figures. In
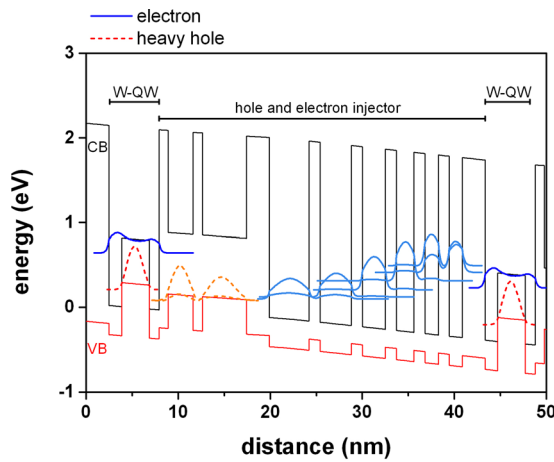
FIG. 1. Band structure of conduction and valence band for one and a half stages, containing two W-QWs and the respective hole and electron injector. Dashed (solid) lines depict the absolute moduli square of heavy hole (electron) wave functions at the W-QW as well as at the injector region.
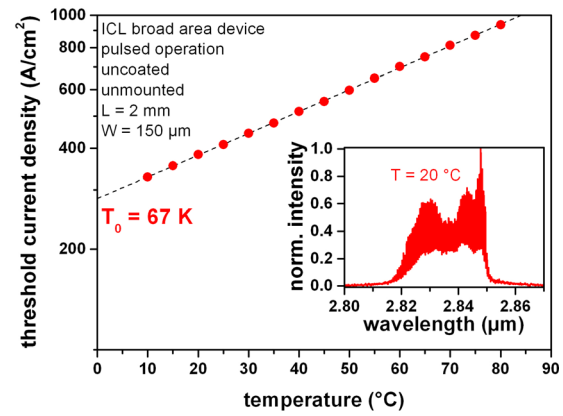

FIG. 2. Temperature dependence of the threshold current density for a broad area device (dimensions: $2\,mm \times 150\,\mu m$) measured in pulsed operation (1 kHz, 250 ns). The threshold current density is $383\,A/cm^2$ at $T = 20\,^\circ C$, and the characteristic temperature T_0 has a value of 67 K. The inset shows a room temperature spectrum with peak wavelength around $2.84\,\mu m$.

addition, narrow RWG structures were patterned by optical lithography and RIE in combination with a Si_3N_4/SiO_2 passivation layer. These devices were tested in cw mode. Finally, DFB devices were processed in a similar fashion. To achieve spectrally single-mode emission, electron beam defined metal gratings were deposited at the sides of the ridges for longitudinal mode selection.[20] It is important to etch below the active region to reduce current spreading and hence increase performance. However, grating coupling decreases rapidly after the last cascade of the active region.[24] Therefore, it is crucial to reach an appropriate etch depth within the lower SCL layer. For passivation of the structures, Si_3N_4 and SiO_2 layers were used again. Contact windows were etched into the passivation layers on top of the ridges by a CHF_3 based reactive ion etch process. Top contact metallization was sputtered, and an additional $10\,\mu m$ Au layer was electroplated to achieve sufficient heat removal. After thinning the substrate to $150\,\mu m$ and applying bottom contact layers, the sample was cleaved into bars with cavity lengths of $900\,\mu m$. The devices were coated using a 30 nm Al_2O_3 passivation layer on the front facet and a metal based high reflectivity mirror on the back facet. The devices were mounted epitaxial-side-up on AlN heat spreaders, which were subsequently soldered onto thermoelectrically cooled TO housings. The TO headers were hermetically sealed using steel caps with anti-reflection coated windows. The DFB devices were then analyzed in cw mode concerning temperature dependent L-I-V characteristics and spectral properties.

Broad area laser devices showed a threshold current density (J_{th}) of $383\,A/cm^2$ at $T = 20\,^\circ C$ [see Fig. 2], which is only slightly higher than reported values for broad area devices based on ICL material with emission wavelength above $3\,\mu m$.[1,15] The characteristic temperature (T_0) obtained from an exponential fit to $J_{th}(T)$ was calculated to 67 K [see Fig. 2], which is the highest value reported based on ICL material so far.[15,25] The inset shows a room temperature spectrum with a peak wavelength around $2.84\,\mu m$. Mounted RWG devices with cavity lengths of 3 mm and ridge widths of $7.8\,\mu m$ showed output powers of >11 mW at $20\,^\circ C$ and laser emission was observed up to $50\,^\circ C$, as shown in Fig. 3.

For the DFB devices with emission wavelength around $2.8\,\mu m$, output powers of a few milliwatts and cw operation at room temperature were observed. Fig. 4(a) shows temperature dependent L-I-V characteristics with a room temperature threshold current density of $1.4\,kA/cm^2$. Considering cw operation around room temperature for devices in this wavelength range, the presented ICL devices are almost comparable to conventional diode lasers.[26] Furthermore, the threshold power density of $6.2\,kW/cm^2$ at $T = 20\,^\circ C$ is much lower than the one of best InP based QCLs.[27] For spectral characterization, a Fourier transform infrared spectrometer with a resolution of $0.125\,cm^{-1}$ was used. The devices showed a wide mode-hop free tuning range of 7 nm (12 nm) with current (current and temperature) which is more than sufficient for most TLAS applications. Tuning rates of 21 nm/W (0.13 nm/mA) with electrical driving power (driving current) and 0.29 nm/K with temperature were extracted. The corresponding thermal resistance-area product extracted from the data presented in Fig. 4(b) is calculated to $3.0\,Kcm^2/kW$. By a variation of the DFB grating period, a wavelength range of more than 150 nm ranging from 2777.5 nm to 2928.8 nm was accessed, effectively covering a
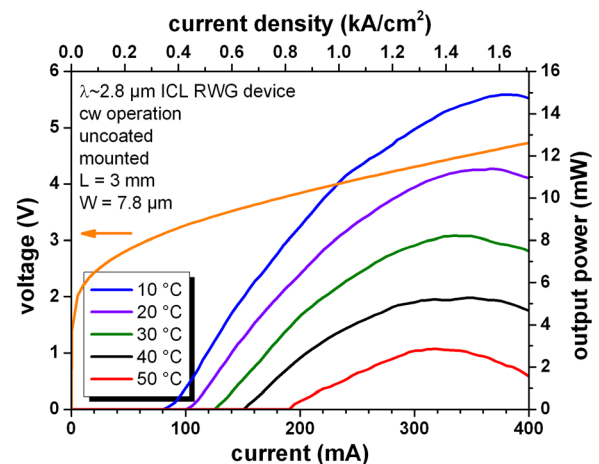

FIG. 3. L-I-V characteristics for a narrow ridge device (dimensions: 3 mm × $7.8\,\mu m$), operated in cw mode. Output powers lie above 10 mW at room temperature, and the maximum operation temperatures is $50\,^\circ C$.
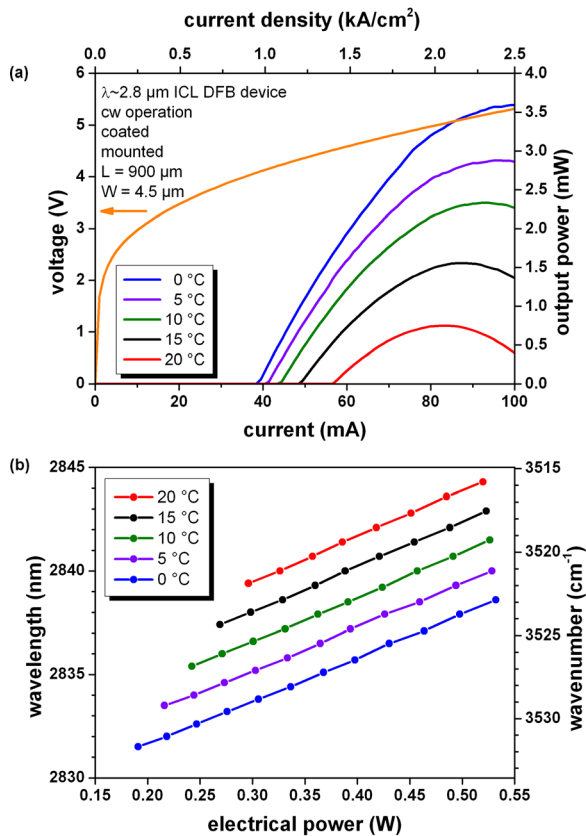
FIG. 4. (a) L-I-V characteristics of an ICL DFB device at temperatures ranging from $0\,°C$ to $20\,°C$ in cw operation. (b) Respective tuning diagram, showing the range of single-mode operation. The current tuning amounts to 7 nm at $0\,°C$, and the overall tuning range is more than 12 nm. Tuning rates of 21 nm/W and 0.29 nm/K were derived.

broad part of the gain bandwidth. Fig. 5 shows the two respective single-mode spectra and a superimposed spectrum of the amplified spontaneous emission of a 1.2 mm long RWG device operated slightly below threshold. The inset
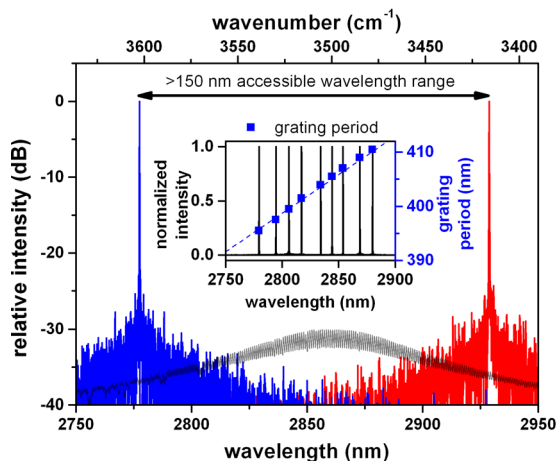

FIG. 5. Single-mode emission spectra of two DFB devices with different grating periods, showing setup limited signal to noise ratios of around 25 dB. A semi-logarithmic amplified spontaneous emission spectrum is superimposed. A wavelength range of more than 150 nm is covered based on the available gain bandwidth of the underlying ICL material used for device processing. The inset depicts single-mode emission spectra recorded at fixed operating conditions of $T_{op} = 10\,°C$ and $I_{op} = 60$ mA for various DFB devices fabricated on identical epitaxial ICL material. The right axis and blue squares depict the different grating periods of each device indicating a respective effective refractive index n_{eff} of 3.51.

depicts spectra (black) and the emission wavelengths of DFB devices against their grating periods (blue squares) operated at identical conditions ($T_{op} = 10\,°C$, $I_{op} = 60$ mA). The emission wavelength λ_{DFB} corresponds to the grating period Λ via the Bragg Condition $\lambda_{DFB} = 2 \cdot n_{eff} \cdot \Lambda$, from which an effective refractive index n_{eff} of 3.51 was derived.

In conclusion, laser emission below $2.8\,\mu m$ based on interband cascade lasers was demonstrated with a record value of the characteristic temperature T_0 of 67 K. Based on pulsed mode operation around room temperature in the wavelength range around $3\,\mu m$, the three earlier mentioned approaches can be compared in terms of threshold current densities: Cascaded type-I QW devices were published with around $100\,A/cm^2$ for quinary diode lasers[8,9] and with around $300\,A/cm^2$ for a superlattice design.[10] Based on QCL technology, threshold current densities of around $2.0\,kA/cm^2$ and $3.5\,kA/cm^2$ were achieved on the InP and InAs material system, respectively.[12,16,28] Despite the presented ICLs being the first attempt towards wavelengths below $3\,\mu m$, their performance is with $383\,A/cm^2$ already comparable to the above mentioned technologies. RWG devices with uncoated facets operating at room temperature show cw output powers around 11 mW. DFB devices operating in cw mode from $0\,°C$ to $20\,°C$ have been demonstrated with a current tuning range of 7 nm, which is very suitable for TLAS application. The ICL approach keeps expanding its usability and will be a convenient tool for a variety of applications.

[1]I. Vurgaftman, W. W. Bewley, C. L. Canedy, C. S. Kim, M. Kim, C. D. Merritt, J. Abell, and J. R. Meyer, IEEE J. Sel. Top. Quantum Electron. **19**, 1200210 (2013).
[2]J. H. Miller, Y. A. Bakhirkin, T. Ajtai, F. K. Tittel, C. J. Hill, and R. Q. Yang, Appl. Phys. B **85**, 391 (2006).
[3]S. Lundqvist, P. Kluczynski, R. Weih, M. v. Edlinger, L. Nähle, M. Fischer, A. Bauer, S. Höfling, and J. Koeth, Appl. Opt. **51**, 6009 (2012).
[4]P. Kluczynski and S. Lundqvist, U.S. patent application No. 13/901,260 (23 May 2013).
[5]G. Wysocki, Y. Bakhirkin, S. So, F. K. Tittel, C. J. Hill, R. Q. Yang, and M. P. Fraser, Appl. Opt. **46**, 8202 (2007).
[6]A. Bauer, K. Rößner, T. Lehnhardt, M. Kamp, S. Höfling, L. Worschech, and A. Forchel, Semicond. Sci. Technol. **26**, 014032 (2011).
[7]K. Vizbaras and M. C. Amann, Semicond. Sci. Technol. **27**, 032001 (2012).
[8]L. Shterengas, R. Liang, G. Kipshidze, T. Hosoda, S. Suchalkin, and G. Belenky, Appl. Phys. Lett. **103**, 121108 (2013).
[9]L. Shterengas, R. Liang, G. Kipshidze, T. Hosoda, G. Belenky, S. S. Bowman, and R. L. Tober, Appl. Phys. Lett. **105**, 161112 (2014).
[10]Y. Jiang, L. Li, R. Q. Yang, J. A. Gupta, G. C. Aers, E. Dupont, J. M. Baribeau, X. Wu, and M. B. Johnson, Appl. Phys. Lett. **106**, 041117 (2015).
[11]T. Lehnhardt, M. Hümmer, K. Rößner, M. Müller, S. Höfling, and A. Forchel, Appl. Phys. Lett. **92**, 183508 (2008).
[12]N. Bandyopadhyay, Y. Bai, S. Tsao, S. Nida, S. Slivken, and M. Razeghi, Appl. Phys. Lett. **101**, 241110 (2012).
[13]I. Vurgaftman, R. Weih, M. Kamp, J. R. Meyer, C. L. Canedy, C. S. Kim, M. Kim, W. W. Bewley, C. D. Merritt, J. Abell, and S. Höfling, J. Phys. D: Appl. Phys. **48**, 123001 (2015).
[14]G. Ryu, A. N. Chryssis, J. Amirloo, S. Saini, F. J. Towner, and M. Dagenais, IEEE Photonics J. **4**, 133–142 (2012).
[15]R. Weih, M. Kamp, and S. Höfling, Appl. Phys. Lett. **102**, 231123 (2013).
[16]B. Hinkov, A. Bismuto, Y. Bonetti, M. Beck, S. Blaser, and J. Faist, Electron. Lett. **48**, 646 (2012).

[17]C. S. Kim, M. Kim, J. Abell, W. W. Bewley, C. D. Merritt, C. L. Canedy, I. Vurgaftman, and J. R. Meyer, Appl. Phys. Lett. **101**, 061104 (2012).

[18]C. S. Kim, M. Kim, W. W. Bewley, J. R. Lindle, C. L. Canedy, J. Abell, I. Vurgaftman, and J. R. Meyer, Appl. Phys. Lett. **95**, 231103 (2009).

[19]M. von Edlinger, J. Scheuermann, R. Weih, C. Zimmermann, L. Nähle, M. Fischer, J. Koeth, S. Höfling, and M. Kamp, IEEE Photonics Technol. Lett. **26**, 480 (2014).

[20]R. Weih, L. Nähle, S. Höfling, J. Koeth, and M. Kamp, Appl. Phys. Lett. **105**, 071111 (2014).

[21]C. L. Canedy, W. W. Bewley, J. R. Lindle, J. A. Nolde, D. C. Larrabee, C. S. Kim, M. Kim, I. Vurgaftman, and J. R. Meyer, J. Electron. Mater. **37**, 1780 (2008).

[22]C. L. Canedy, J. Abell, C. D. Merritt, W. W. Bewley, C. S. Kim, M. Kim, I. Vurgaftman, and J. R. Meyer, Opt. Express **22**, 7702 (2014).

[23]I. Vurgaftman, W. W. Bewley, C. L. Canedy, C. S. Kim, M. Kim, C. D. Merritt, J. Abell, J. R. Lindle, and J. R. Meyer, Nat. Commun. **2**, 585 (2011).

[24]Y. B. Wang, Y. Xu, Y. Zhang, G. F. Song, and L. H. Chen, J. Phys. D **45**, 505109 (2012).

[25]I. Vurgaftman, W. W. Bewley, C. D. Merritt, C. L. Canedy, C. S. Kim, J. Abell, J. R. Meyer, and M. Kim, Proc. SPIE **8268**, 82681F (2012).

[26]M. Hümmer, K. Rößner, T. Lehnhardt, M. Müller, A. Forchel, R. Werner, M. Fischer, and J. Koeth, Electron. Lett. **42**, 583 (2006).

[27]M. Razeghi, N. Bandyopadhyay, Y. Bai, Q. Lu, and S. Slivken, Opt. Mater. Express **3**, 1872 (2013).

[28]P. Laffaille, J. C. Moreno, R. Teissier, M. Bahriz, and A. N. Baranov, AIP Adv. **2**, 022119 (2012).